COMPARATIVE NUMERICAL ANALYSIS OF DIESEL AND BIODIESEL COMBUSTION IN AN INTERNAL COMBUSTION ENGINE

by

Habib BOUIGHI[a], Hamza BOUSBAA[a], Younes MENNI[b,c], Mustafa BAYRAM[d*], Omolayo M. IKUMAPAYI[e], Abiodun BAYODE[e], and Tin Tin TING[f,g]

[a] Laboratory of Environmental Technology Research, Department of Mechanical Engineering, Faculty of Sciences and Technology, ENP MA-Oran, Oran, Algeria, Algeria
[b] Department of Mechanical Engineering, Institute of Technology, University Center Salhi Ahmed Naama, Naama, Algeria
[c] College of Technical Engineering, National University of Science and Technology, Dhi Qar, Iraq
[d] Department of Computer Engineering, Biruni University, Istanbul, Turkey
[e] Department of Mechanical Engineering, Northwest University, Potchefstroom, South Africa
[f] Faculty of Data Science and Information Technology, INTI International University, Nilai, Malaysia
[g] School of Information Technology, UNITAR International University, Selangor, Malaysia

Original scientific paper
https://doi.org/10.2298/TSCI2504123B

This study presents a comprehensive numerical investigation comparing the combustion characteristics and emission behavior of conventional diesel and biodiesel fuel (methyl oleate, $C_{19}H_{38}O_2$) in a single-cylinder Antor 6LD400 Diesel engine using CONVERGE CFD software. The simulations were carried out under identical operating conditions to evaluate temperature and pressure evolution, heat release profiles, and pollutant formation, including CO, CO_2, NO_x, soot, and unburned hydrocarbons. Results indicate that biodiesel ignites earlier due to its higher cetane number and oxygenated structure, leading to faster combustion, lower peak in-cylinder pressure and temperature, and reduced emissions of CO, hydrocarbon, and soot. Although biodiesel emits slightly more CO_2, indicative of more complete combustion, it consistently demonstrates lower NO_x levels due to shorter residence time at high temperatures. These findings confirm that biodiesel offers cleaner combustion with significant emission benefits, making it a promising alternative fuel for reducing the environmental impact of compression ignition engines.

Key words: *biodiesel, methyl oleate, diesel engine, combustion, emissions*

Introduction

Increasing environmental pressures and the finite nature of fossil fuel resources have intensified efforts to identify cleaner, renewable alternatives for compression ignition (CI) engines. Biodiesel, derived from sustainable feedstocks, has emerged as a promising candidate due to its ability to lower emissions of CO, HC, and PM, while also offering improved lubricity and compatibility with existing Diesel engines, as highlighted by Yilmaz and Vigil [1] and Hoekman *et al*. [2]. Extensive reviews and experiments have explored biodiesel's combustion, performance, and emission behavior across a variety of feedstocks and enhancement tech-

* Corresponding author, e-mail: mustafabayram@biruni.edu.tr

niques, [3-10]. Nevertheless, biodiesel use presents challenges such as increased viscosity, reduced volatility, and elevated NO_x emissions. To overcome these drawbacks, several strategies have been proposed. Hydrogen enrichment has demonstrated benefits in improving combustion efficiency and reducing pollutant output, [3, 5, 8, 10, 11], while the application of nanoand ternary additives has enhanced atomization, reduced ignition delay, and accelerated combustion kinetics, [12-17]. Intake and exhaust modifications, such as exhaust gas re-circulation, water injection, and boost pressure control, have also contributed to emission reduction and improved thermal management, [11, 18, 19]. Furthermore, optimizing injection parameters and adopting non-circular orifices have improved spray characteristics, leading to better fuel-air mixing and combustion efficiency, [4, 13, 20]. In this context, computational tools such as CFD have become essential for analyzing in-cylinder combustion phenomena, providing insights into heat release, pollutant formation, and engine optimization strategies, [9, 14, 21].

This study is motivated by the need to better understand and improve the combustion behavior of biodiesel as a cleaner alternative to diesel fuel. The aim is to numerically compare the in-cylinder combustion characteristics of diesel and methyl oleate biodiesel using CONVERGE CFD (Version 3), with a focus on pressure-temperature evolution, combustion efficiency, and emission formation (CO, CO_2, NO_x, and soot), to support the development of more sustainable engine technologies.

Engine specifications and simulation set-up

This study numerically investigates the combustion performance of conventional diesel and biodiesel, specifically methyl oleate ($C_{19}H_{38}O_2$), in the Antor 6LD400 single-cylinder diesel engine [20]. The simulation evaluates pressure and temperature evolution, heat release, and emissions (CO, CO_2, NO_x, HC, and soot) under identical operating conditions. This engine model features an 86 mm bore, a 68 mm stroke, a compression ratio of 18:1, and a displacement of 395 cm³. It is equipped with a direct injection system operating at 24° bTDC, using a 0.24 mm × 4 hole × 160° nozzle. The rated power output is 5.4 kW at 3000 rpm.

The physical and chemical properties of the fuels are adopted from the literature. Conventional diesel, as characterized by Bousbaa *et al*. [22], has a density of 852 kg/m³ at 15 °C, a viscosity of 1.57 mPa·s at 40 °C, a lower heating value (LHV) of 42.80 MJ/kg, and a cetane number of 55. It contains 86 wt.% carbon and 14 wt.% hydrogen. In contrast, methyl oleate, based on Hasnain *et al*. [23], exhibits a density of 859.02 kg/m³, a viscosity of 4.34 mm²/s, and a lower LHV of 37.05 MJ/kg. It has a higher cetane number of 58.11 and is composed of 77.32 wt.% carbon, 11.38 wt.% hydrogen, and 11.30 wt.% oxygen, providing inherent oxygenation that can promote cleaner combustion.

The simulations are performed using a compressible, unsteady RANS framework, assuming an ideal gas behavior. The governing equations include [24]:

– Continuity equation for species *m*

$$\frac{\partial \rho_m}{\partial t} + \nabla\left(\rho_m u\right) = \nabla\left[\rho D \nabla\left(\frac{\rho_m}{\rho}\right)\right] + \dot{\rho}_m^c + \dot{\rho}^s \delta_{m1} \tag{1}$$

– Total mass continuity equation (summing over all species)

$$\frac{\partial \rho}{\partial t} + \nabla\left(\rho u\right) = \dot{\rho}^s \tag{2}$$

– Momentum equation

$$\frac{\partial\left(\rho u\right)}{\partial t} + \nabla\left(\rho u u\right) = -\frac{1}{a^2}\nabla p - A_0\left(\frac{2}{3}\rho k\right) + \nabla\sigma + F^s + \rho g \tag{3}$$

– Internal energy conservation equation

$$\frac{\partial(\rho I)}{\partial T}+\nabla(\rho u I)=-p\nabla u-\nabla J+(1-A_0)\sigma:\nabla u+A_0\rho\varepsilon+\dot{Q}^c+\dot{Q}^s \tag{4}$$

where ρ is the fluid density, ρ_m – the mass density of species m, u – the velocity vector, p – the pressure, D – the diffusion coefficient, σ – the stress tensor, I – the internal energy, J – the heat flux, g – the gravitational acceleration, A_0 – the turbulence interaction constant, k – the turbulent kinetic energy, ε – the dissipation rate, $\dot{Q}^c$ and $\dot{Q}^s$ – the heat sources from combustion and spray, while $\dot{\rho}_m^c$ and $\dot{\rho}^s$ – the corresponding mass sources. The δ_{m1} ensures species-specific source terms.

Simulations are performed at 1600 rpm to represent moderate load conditions. Initial conditions inside the combustion chamber are set at a pressure of 1.036 bar and a temperature of 355 K. Wall boundary conditions are defined by setting the cylinder head, cylinder wall, and piston temperatures to 523 K, 433 K, and 553 K, respectively [24].

A structured mesh ranging from 32460-920540 cells was generated to match the combustion chamber geometry, as illustrated in fig. 1. Refinement was applied near the injector, piston bowl, and flame front using adaptive mesh refinement (AMR) based on gradients of velocity, temperature, and species concentration. This meshing strategy enhances resolution in regions with steep gradients while maintaining overall computational efficiency.

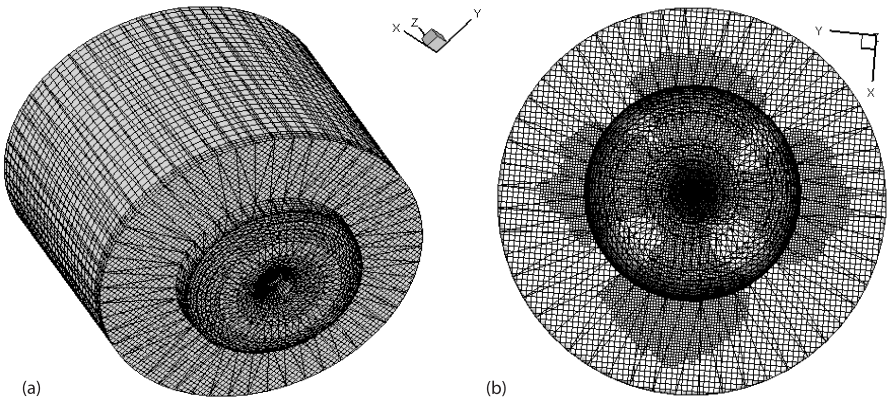

Figure 1. (a) Mesh of the domain and (b) an AMR in the combustion chamber

The simulation employed the finite volume approach with second-order accuracy to solve the governing equations. Turbulence effects were captured using the RNG k-ε model [25], while the KH-RT model [26] was used to describe the fuel spray breakup process. Combustion was simulated using the CTC model [27] coupled with the Shell ignition model [28], while emissions were predicted using the extended Zeldovich model for NO_x [26] and the Hiroyasu model for soot [29].

The numerical model was validated by comparing the simulated in-cylinder pressure profile with experimental data for the Antor

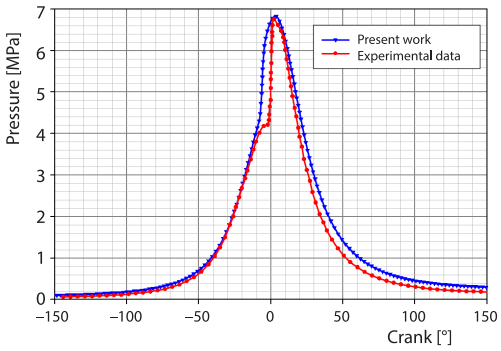

Figure 2. Simulated *vs.* experimental cylinder pressure in the Antor 6LD400 engine [20]

6LD400 Diesel engine, as reported by Bayramoglu and Nuran [20]. As shown in fig. 2, the simulation was performed using conventional diesel under the same operating conditions as the experiment. The predicted pressure curve closely matches the experimental data in terms of ignition timing, peak pressure magnitude, and pressure evolution, thereby confirming the reliability and accuracy of the simulation set-up and combustion modelling approach used in this study.

Results and analysis

Figure 3 presents a comparative analysis of in-cylinder temperature and pressure profiles for diesel and methyl oleate biodiesel during the engine cycle. In fig. 3(a), the biodiesel curve shows an earlier rise in temperature compared to the diesel curve, indicating a shorter ignition delay. This behavior is attributed to biodiesel's higher cetane number (58.11 *vs*. 55 for diesel), which promotes faster autoignition. Despite earlier combustion, diesel reaches a slightly higher peak temperature due to its greater LHV (42.80 MJ/kg *vs*. 37.05 MJ/kg for biodiesel), which results in more thermal energy release. The oxygen content in biodiesel (11.30 wt.%) contributes to more complete and cleaner combustion but also leads to lower flame temperatures. In contrast, diesel combustion occurs later but sustains a longer heat release, as evidenced by its broader temperature profile.

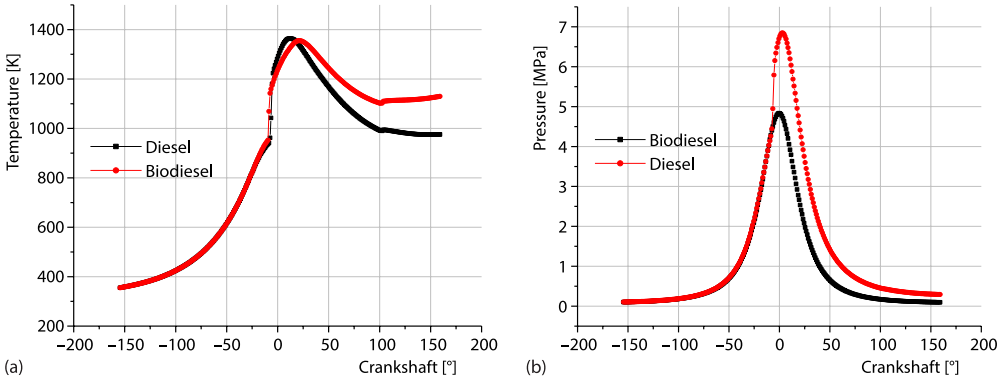

Figure 3. Combustion comparison of diesel and biodiesel; (a) temperature *vs*. crank angle and (b) cylinder pressure variation

In fig. 3(b), the pressure evolution confirms the observed combustion trends: biodiesel exhibits an earlier pressure rise due to its shorter ignition delay. In contrast, diesel reaches a slightly higher peak pressure, which aligns with its higher energy density. The combustion of biodiesel is more abrupt, as evidenced by a steeper pressure increase, while diesel combustion proceeds more gradually with a slower pressure buildup. These results clearly demonstrate that biodiesel combusts earlier and more rapidly, with slightly lower peak pressure and temperature, consistent with its physical and chemical properties, including higher viscosity, LHV, and oxygenated molecular structure.

Figure 4 compares the heat release characteristics of diesel and biodiesel (methyl oleate) by analyzing both instantaneous and cumulative heat release as functions of crank angle. As observed in fig. 4(a), biodiesel initiates heat release earlier than diesel, signifying a reduced ignition delay. This behavior is primarily linked to biodiesel's higher cetane number and its oxygenated molecular structure, which enhance autoignition tendencies and facilitate more complete fuel oxidation. The peak heat release rate for biodiesel occurs ear-

lier and is sharper, reflecting a more concentrated combustion event over a narrower crank angle range. In contrast, diesel shows a slightly higher peak, owing to its greater LHV (42.80 MJ/kg *vs*. 37.05 MJ/kg for biodiesel), resulting in more thermal energy released per unit mass. The broader profile of the diesel HRR indicates a longer combustion duration.

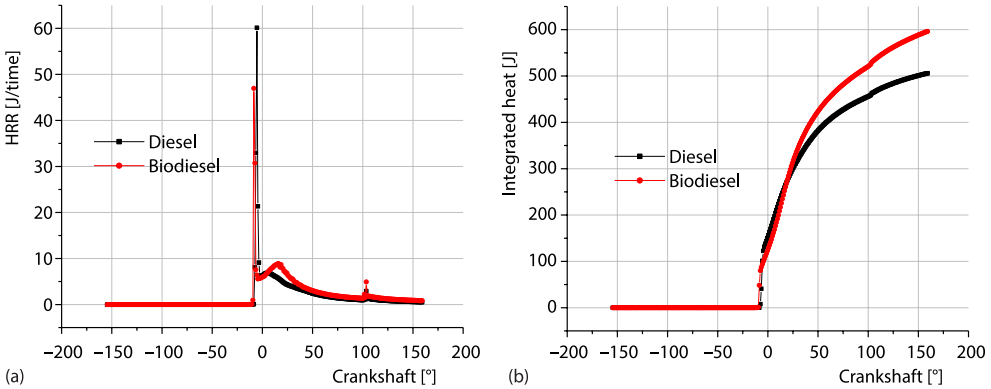

Figure 4. Heat release analysis of diesel and biodiesel, (a) instantaneous heat release rate and (b) cumulative heat release

In fig. 4(b), the cumulative heat release curve for biodiesel rises earlier and more steeply than that of diesel, confirming faster combustion and earlier energy delivery. However, diesel ultimately achieves a higher total cumulative heat release, consistent with its higher energy density. These results illustrate that biodiesel combusts earlier and faster, while diesel combustion is more gradual but delivers more energy overall. This difference in heat release behavior highlights biodiesel's potential for cleaner and more efficient combustion, with implications for combustion phasing, thermal efficiency, and emission formation.

Figures 5(a) and 5(b) present a comparison of the CO and CO_2 emission profiles for diesel and biodiesel (methyl oleate), respectively, during the combustion process. Diesel produces significantly higher CO emissions, primarily due to its lack of intrinsic oxygen, which limits oxidation in locally rich zones and results in incomplete combustion. In contrast, biodiesel, with approximately 11.30 wt.% oxygen in its molecular structure, promotes more complete oxidation of intermediate species such as CO into CO_2. This effect is further supported by biodiesel's higher cetane number and earlier combustion phasing, as observed in figs. 3 and 4, which allow more time for oxidation within the cylinder and lead to reduced CO accumulation. Complementary to this, biodiesel exhibits slightly higher CO_2 emissions, reflecting a more complete carbon oxidation process. Although diesel contains a higher carbon content (86 wt.%) compared to biodiesel (77.32 wt.%), its lower CO_2 output suggests less efficient combustion. These results, taken together, confirm that biodiesel achieves cleaner and more complete combustion than diesel under identical engine conditions, reinforcing its suitability as a sustainable and environmentally favorable alternative to conventional fossil diesel.

Figure 5(c) presents the NO_x emission profiles for diesel and biodiesel (methyl oleate), revealing that diesel produces noticeably higher NO_x levels throughout the combustion cycle. This trend is primarily attributed to diesel's higher peak in-cylinder temperatures, as shown in fig. 3(a), which promote thermal NO_x formation through the extended Zeldovich mechanism. Additionally, diesel's slower combustion and longer residence time at elevated temperatures further contribute to increased NO_x generation. In contrast, biodiesel exhibits lower NO_x emis-

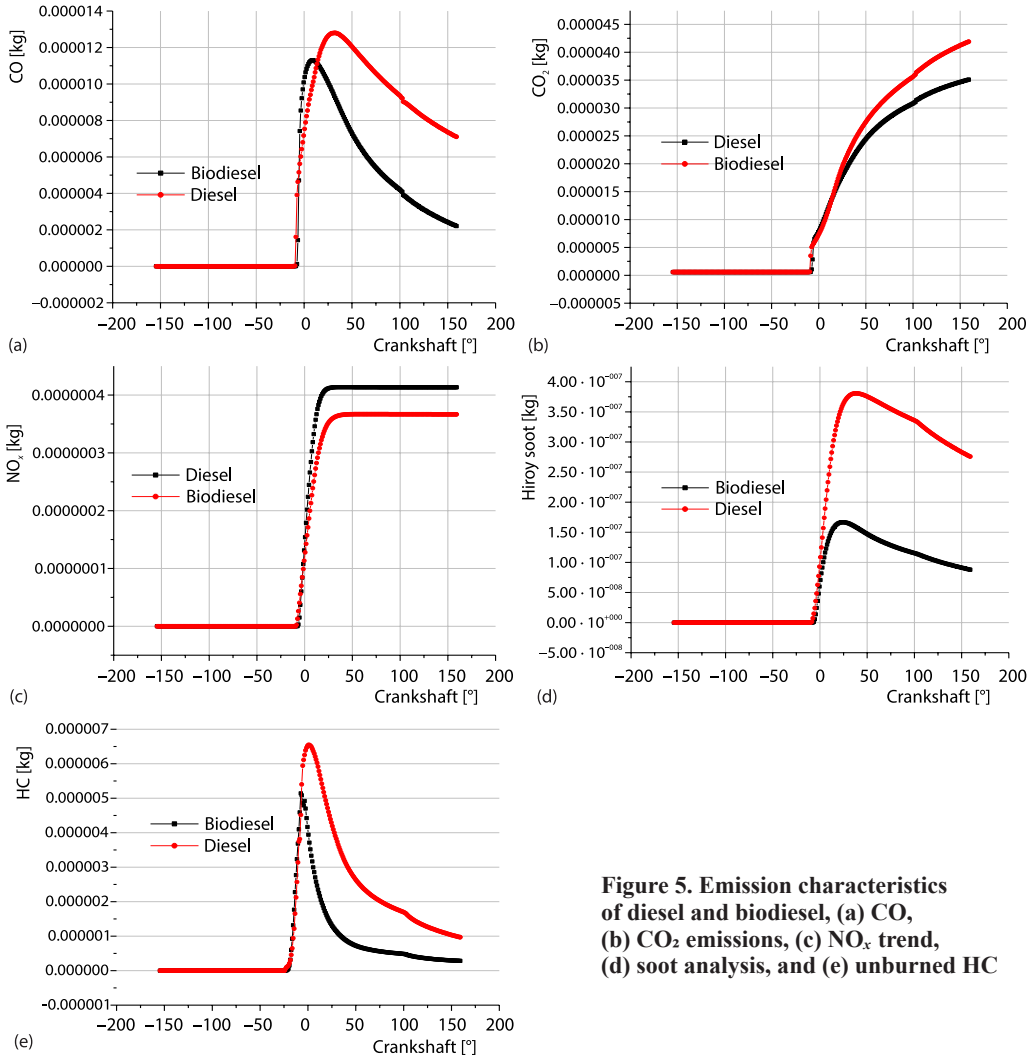

Figure 5. Emission characteristics of diesel and biodiesel, (a) CO, (b) CO_2 emissions, (c) NO_x trend, (d) soot analysis, and (e) unburned HC

sions despite its higher oxygen content. This reduction is due to its lower calorific value, which leads to reduced peak temperatures, and its faster combustion process, which limits the duration of high temperature exposure necessary for NO_x formation. The earlier ignition and shorter combustion duration of biodiesel further restrict NO_x production.

Figures 5(d) and 5(e) present the soot and unburned HC emission profiles for diesel and biodiesel (methyl oleate) throughout the combustion cycle. Diesel produces significantly higher soot emissions, primarily due to its higher carbon content (86 wt.%) and lack of inherent oxygen, which lead to locally fuel-rich zones and incomplete combustion, conditions favorable for soot precursor formation. In contrast, biodiesel contains 11.30 wt.% oxygen in its molecular structure, promoting in-cylinder oxidation even in areas with limited air-fuel mixing. This facilitates the early oxidation of soot precursors, limiting their growth into larger particles. Additionally, biodiesel's faster combustion and shorter residence time at high temperatures further reduce nucleation, surface growth, and agglomeration of soot. Although diesel reaches

slightly higher peak combustion temperatures, these are insufficient to offset the extended soot formation window during its longer combustion phase. Biodiesel interrupts this process more effectively through its oxygen-rich and cleaner-burning characteristics. Similarly, diesel exhibits noticeably higher HC emissions due to longer ignition delay, suboptimal fuel-air mixing, and lack of fuel-bound oxygen, leading to partial combustion, particularly in crevices and quench zones. Biodiesel, by contrast, ignites earlier and burns more completely due to its higher cetane number and oxygenated structure, which reduce the occurrence of unburned hydrocarbons. Improved atomization and enhanced mixing associated with its higher viscosity also contribute to lower HC emissions. These results are consistent with earlier observations in figs. 3 and 4 and further demonstrate biodiesel's advantage in minimizing soot and HC formation.

Conclusions

This study performed a comprehensive numerical analysis using CONVERGE CFD to compare the combustion and emission behavior of conventional diesel and biodiesel, with methyl oleate as the representative oxygenated fuel, in a single-cylinder compression ignition engine. The conclusions are as fpllows.

- Methyl oleate biodiesel exhibited earlier ignition and more rapid combustion, attributed to its higher cetane number and oxygenated molecular structure, which resulted in reduced ignition delay and a more concentrated heat release.
- While diesel exhibited marginally higher peak in-cylinder pressure and temperature as a result of its higher LHV, biodiesel demonstrated superior combustion completeness, indicated by higher CO_2 emissions and lower concentrations of CO and unburned hydrocarbons.
- The NO_x emissions were lower for biodiesel, primarily due to its lower flame temperatures and shorter residence time in high temperature zones, despite its oxygenated nature.
- Soot formation was significantly reduced during biodiesel combustion, owing to enhanced oxidation pathways facilitated by the fuel-bound oxygen and improved fuel-air mixing.

Methyl oleate biodiesel showed cleaner combustion and lower emissions, confirming its viability as a sustainable diesel alternative. Further research should explore its performance under varied engine loads, fuel blends, and injection strategies.

References

[1] Yilmaz, N., Vigil, F. M., Potential Use of a Blend of Diesel, Biodiesel, Alcohols and Vegetable Oil in Compression Ignition Engines, *Fuel*, *124* (2014), May, pp. 168-172
[2] Hoekman, S. K., *et al*., Review of Biodiesel Composition, Properties, and Specifications, *Renewable and Sustainable Energy Reviews*, *16* (2012), 1, pp. 143-169
[3] Equbal, M. N., *et al*., Advances in Hydrogen-Enriched Biogas/Biodiesel Combustion for Near-Zero Emissions in Direct Injection Engines, *International Journal of Thermofluids*, *27* (2025), 101269
[4] Yadav, M., *et al.*, Enhancing Combustion and Emission Characteristics of CI Engines through Atomization and Fuel-Air Mixing Using Non-Circular Orifices: A Path Towards Sustainable Biodiesel Utilization, *Green Technologies and Sustainability*, *3* (2024), 3, 100161
[5] Kumar, V., Choudhary, A. K., A Comparative Review on Evaluation of Performance, Combustion, and Emission Characteristics of Biodiesel Blends Enriched with Hydrogen, Additives and Their Combined Effect, *Thermal Science and Engineering Progress*, *46* (2023), 102185
[6] Celebi, Y., *et al*., Biofuel Usage in Diesel Engines Powered By Butanol and Its Blends: A review, *Fuel, 387* (2025), 134316
[7] Al-Hwaiti, M., *et al*., Effect of Catalysts On Performance and Emission in a Combustion Diesel Engine Using Biodiesel Derived from Non-Edible Plant "Handal": Case study in Jordan, *Energy*, *321* (2025), 135432
[8] Hariram, V., *et al*., Enhanced Combustion and Emission Characteristics of Diesel-Algae Biodiesel-Hydrogen Blends in a Single-Cylinder Diesel Engine, *Results in Engineering*, *26* (2025), 104676

[9] Akintunde, S. B., *et al.*, Numerical and Experimental Studies on Combustion of Hura Crepitans Biodiesel-Diesel Blends in a Compression Ignition (CI) Engine, *Thermal Advances*, *2* (2025), 100012
[10] Lakshmikanth, G., *et al*., Performance, Combustion, and Emission Evaluation of Cassia Fistula Biodiesel Blends with Hydrogen Induction in a Low Heat Rejection Diesel Engine, *International Journal of Hydrogen Energy*, *143* (2025), July, pp. 468-478
[11] Vellaiyan, S., Optimization of Hydrogen-Enriched Biodiesel-Diesel Dual-Fuel Combustion with EGR for Sustainable Engine Performance, *International Journal of Hydrogen Energy*, *128* (2025), May, pp. 85-94
[12] Mofijur, *et al.*, Impact of Nanoparticle-Based Fuel Additives on Biodiesel Combustion: An Analysis of Fuel Properties, Engine Performance, Emissions, and Combustion Characteristics – A Review, *Energy Conversion and Management, X* (2024), 21, 100515
[13] Srinivasan, D. R., *et al.*, A Hybrid Approach to Optimize Engine Performance and Emission Control in Internal Combustion Engines Using Graphene Quantum Dots-Enhanced Biodiesel-Diesel Blends, *Applied Thermal Engineering*, *276* (2025), 126841
[14] Hamzah, A. H., *et al*., Effect of Nanoparticles and Biodiesel Blended with Diesel on Combustion Parameters in Compression Ignition Engine: Numerical Analysis, *Energy Engineering*, *122* (2025), 5, pp. 2059-2075
[15] Kumar, K., *et al*., Effect of TiO_2 Nanoparticles and Hydrogen on the Combustion, Performance, and Emissions of Madhuca Biodiesel in a Diesel Engine, *International Journal of Hydrogen Energy*, *143* (2025), July, pp. 635-649
[16] Dhamodaran, G., Elumalai, A., Effect of ternary Nanocomposite in Margosa Biodiesel Microemulsion Blends on Performance, Emission, and Combustion Characteristics of a Diesel Engine, *Energy*, *326* (2025), 136362
[17] Kul, V. S., *et al*., Investigation of the Effect of Utilisation of Nanoboron, Diesel and Biodiesel Fuels with Together Hydrogen in a Compression Ignition Engine on Combustion Characteristics, *International Journal of Thermofluids*, *27* (2025), 101232
[18] Manesh, M. M., *et al*., Comparative Analysis of Water Injection and EGR Effects on Combustion, Performance, and Emission Characteristics of a Diesel Engine Using Diesel-Biodiesel Blends, *Cleaner Engineering and Technology*, *26* (2025), 100965
[19] Soyler, H., Boost Pressure Influence on Combustion, Emission Characteristics, and Performance of Diesel Engines with Various Fuel Types, *Engineering Science and Technology, an International Journal*, *63* (2025), 101983
[20] Bayramoglu, K., Nuran, M., Analyzing the Effect of Fuel Injection Timing and Injection Duration on Performance and Emissions in Diesel Engines, *Journal of ETA Maritime Science*, *8* (2020), 1, pp. 38-52
[21] Abdou, B. N., *et al.*, Engine Roughness, Block Vibration and External Noise of Diesel Engine Running on Jojoba Biodiesel and Diesel Blends, *International Journal of Thermofluids*, *27* (2025), 101236
[22] Bousbaa, H., *et al*., Prediction and Simulation of Biodiesel Combustion in Diesel Engines: Evaluating Physicochemical Properties, Performance, and Emissions, *Fire*, *7* (2024), 10, 364
[23] Hasnain, S. M., *et al*., Investigation and Impact Assessment of Soybean Biodiesel, Methyl Oleate, and Diesel Blends on CRDI Performance and Emissions, *Materials Science for Energy Technologies*, *7* (2024), 1 pp. 124-132
[24] Bousbaa, H., *et al*., Investigations on a Compression Ignition Engine Using Animal Fats and Vegetable Oil As Fuels, *Journal of Energy Resources Technology*, *134* (2012), 022202-1
[25] Han, Z., Reitz, R. D., Turbulence Modelling of Internal Combustion Engines Using RNG k-ε Models, *Combustion Science and Technology*, *106* (1995), 4-6, pp. 267-295
[26] Ramos, J. I., *Internal Combustion Engine Modelling*, American Publication Corporation, Hemisphere, Scottsdale, Ariz., USA, 1989
[27] Kong, S. C., *et al*., The Development and Application of a Diesel Ignition and Combustion Model for Multidimensional Engine Simulation, *J. of Engines*, *104* (1995), 3, pp. 502-518
[28] Hamosfakidis, V., Reitz, R. D., Optimization of a Hydrocarbon Fuel Ignition Model for Two Single Component Surrogates of Diesel Fuel, *Combustion and Flame*, *132* (2003), 3, pp. 433-450
[29] Hiroyasu, H., Kadota, T., Models for Combustion and Formation of Nitric Oxide and Soot in Direct Injection Diesel Engines, *SAE Transactions*, (1976), pp. 513-526

Paper submitted: March 2, 2025
Paper revised: April 10, 2025
Paper accepted: June 19, 2025